Deactivation processes of highly excited atomic nitrogen, $N(2p^23p\ ^2S)$

Hironobu Umemoto,* Naoki Terada, Kunikazu Tanaka and Shigeki Oguro

Department of Chemical Materials Science, Japan Advanced Institute of Science and Technology, Asahidai, Tatsunokuchi, Nomi, Ishikawa 923-1292, Japan. E-mail: umemoto@jaist.ac.jp

Received 25th April 2000, Accepted 5th June 2000
Published on the Web 30th June 2000

Rate constants for the deactivation of $N(2p^23p\ ^2S)$ by rare gas atoms and simple molecules were determined. $N(2p^23p\ ^2S)$ was produced by two-photon excitation of $N(2p^3\ ^2D)$ which was produced by the two-photon dissociation of NO. Fluorescence at 149 nm after cascading to $N(2p^23s\ ^2P)$ was monitored to determine the decay rate of $N(2p^23p\ ^2S)$. Except for He and Ne, the rate constants are large, especially for molecular species. For Ar, one of the main exit channels is the production of $N(2p^23s\ ^2P)$. The production efficiency is $26 \pm 3\%$. Such a channel could not be identified for other quenchers. The cross-sections for the quenching by molecular species can be correlated to the long-range interaction parameters.

Introduction

Two-photon laser induced fluorescence (LIF) is a useful technique to monitor the densities of atomic and molecular species which have no absorption in the visible or near ultraviolet region. In this technique, however, care must be paid to the quenching of the upper state, as is the always case for LIF measurements. This is especially important when the radiative lifetime of the upper state is long. $N(2p^3\ ^2D)$, which plays important roles in the upper atmosphere, can easily be detected by the two-photon LIF technique *via* the $2p^23p\ ^2S$ state.[1] Since the radiative lifetime of $N(2p^23p\ ^2S)$ is as long as 102 ns,[2] the information on the quenching rates of $N(2p^23p\ ^2S)$ is necessary to compare the LIF intensities under various conditions. However, there has been no such information. $N(2p^3\ ^2D)$ can also be detected by resonance absorption and resonance enhanced multiphoton ionization (REMPI) techniques.[3–6] The sensitivity of resonance absorption, however, is not as high as those of two-photon LIF and REMPI techniques. Although the sensitivity of REMPI is high, it is difficult to apply this technique in bulk systems.

Copeland *et al.* have measured the rate constants for the quenching of another highly excited atomic nitrogen, $N(2p^23p\ ^4D_{7/2})$, by rare gas atoms and by molecular nitrogen.[7] The rate constants are large for Ar, Kr, Xe and N_2, while they are small for He and Ne. Their results for rare gas atoms can be explained by the difference in the electronic energy levels. The electronic energy of $N(2p^23p\ ^4D_{7/2})$ is 94 882 cm^{-1} which is higher than those of the first excited states of Ar, Kr and Xe, but lower than those of He and Ne. Fig. 1 illustrates the energy level diagram of N, Ar and Kr atoms. The production of electronically excited rare gas atoms should be the main exit channels for Ar, Kr and Xe, while such exit channels are closed for He and Ne. The situation should be similar for $N(2p^23p\ ^2S)$ except for the quenching by Ar. In the case of $N(2p^23p\ ^4D_{7/2})$, there are three exothermic exit channels. Among them, the production of $Ar(3p^54s\ ^3P_0)$ is near resonant. The exothermicity is 328 cm^{-1}.[2] On the other hand, the electronic energy of $N(2p^23p\ ^2S)$, 93 582 cm^{-1}, is a little lower than that of $N(2p^23p\ ^4D_{7/2})$. There is only one exothermic exit channel, the production of $Ar(3p^54s\ ^3P_2)$, the exothermicity of which is 438 cm^{-1}.[2] There may be a difference in the quenching rates by Ar.

In general, the rate constants for the quenching of highly excited atoms by molecular species are large and show minor dependence on the chemical characters such as bond strength.[8–10] However, there are some exceptions. The rate constants for the quenching of excited rare gas atoms by some diatomic molecules, such as H_2 and N_2, are much smaller than those of polyatomic molecules.[9–13] Perfluoroalkanes are not reactive in many systems.[8–11] It is informative to check if a similar tendency can be observed in the quenching of highly excited nitrogen atoms.

Experimental

The experimental apparatus and the procedure were similar to those described elsewhere.[1] NO was two-photon photolyzed to produce $N(2p^3\ ^2D_{5/2})$ with the frequency doubled output of a YAG laser pumped dye laser (Quanta-Ray, GCR-170 and PDL-3) at 275.3 nm. Then, $N(2p^3\ ^2D_{5/2})$ was two-photon excited to $N(2p^23p\ ^2S)$ with the frequency doubled output of another YAG laser pumped dye laser (Quanta-Ray, GCR170 and Lambda Physik, LPD3000E) at 269.0 nm. These two laser beams were aligned collinearly and focused into the interaction region by using 200 mm focal-length lenses. The delay time between the two laser pulses was fixed at 100 ns.

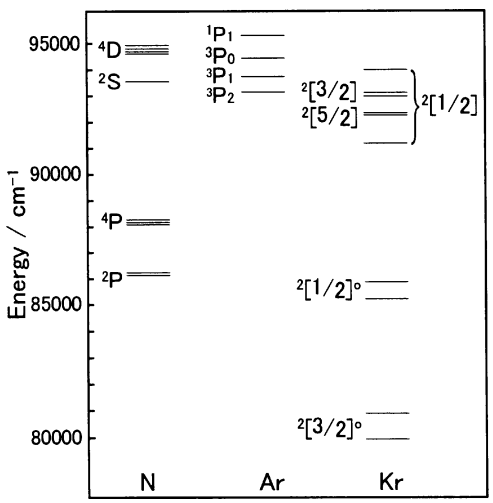

Fig. 1 Energy levels of N, Ar and Kr atoms.

$N(2p^23p\ ^2S)$ atoms are collisionally or radiatively relaxed to the $2p^23s\ ^2P$ state which fluoresces vacuum ultraviolet (VUV) light at 149 nm. The VUV emission was collected through an MgF_2 window and an interference filter (Acton Research, 150-N) and detected with a solar-blind photomultiplier tube (Hamamatsu Photonics, R1459). The photomultiplier signal was monitored and averaged with a digital oscilloscope (LeCroy, 9450A). Since the radiative lifetime of $N(2p^23s\ ^2P)$, 2 ns, is much shorter than that of $N(2p^23p\ ^2S)$, 102 ns,[2] the temporal profile of the VUV emission represents that of the $N(2p^23p\ ^2S)$ population. By measuring the decay profiles as a function of the quencher pressure, it is possible to determine the rate constants for the quenching of $N(2p^23p\ ^2S)$. The gas pressures were measured with capacitance manometers (MKS Baratron, 122AA and Diavac, SG-133K). All the measurements were carried out at room temperature, 295 ± 2 K. The typical pulse energy of the photolysis laser was 8 mJ, while that of the second laser was 1.5 mJ. It should be noted that the decay profiles did not change when the pulse energies of the lasers were halved. This shows that ionization–recombination processes are not important in the present system. The diffusional loss from the viewing zone can be ignored because of the short lifetimes of the upper states.

The rate constants for the deactivation of $N(2p^3\ ^2D_{5/2})$ were also measured for Kr, Xe and CO. The procedure is the same as that described previously.[1] 27 kPa of Ar was added to suppress the diffusional loss.

NO (Sumitomo Seika, 99.999%), He (Teisan, 99.995%), Ne (Teisan 99.99%), Ar (Teisan, 99.9995%), Kr (Nihon Sanso, 99.995%), Xe (Teisan, 99.995%), H_2 (Nihon Sanso, 99.99%), N_2 (Teisan, 99.999%), CO (Takachiho Kako, 99.95%), N_2O (Sumitomo Seika, 99.999%), CH_4 (Nihon Sanso, 99.999%), C_2H_6 (Takachiho Kako, 99.9%), C_3H_8 (Takachiho Kako, 99.9%) and CF_4 (Takachiho Kako 99.999%) were used from cylinders without further purification. Distilled and deionized H_2O was used after being degassed under vacuum.

Results

The rate constants for the deactivation of $N(2p^23p\ ^2S)$ were determined under pseudo-first-order conditions. NO pressure was kept constant, 27 Pa, except for the deactivation rate measurements by NO itself. In this case, NO pressure was changed between 7 and 67 Pa. The reactant pressure was changed between 0 and 40 Pa for efficient quenchers, such as Xe, while it was changed between 0 and 27 kPa for inefficient quenchers such as Ne. The emission intensity from $N(2p^23s\ ^2P)$ decreased exponentially with time. The decay rate increased linearly with the increase in the reactant gas pressure. From such pressure dependence, it is possible to evaluate the rate constants for the deactivation of $N(2p^23p\ ^2S)$. The results are summarized in Table 1. The error limits are the standard deviations (1σ). By extrapolating the NO pressure dependence, the radiative lifetime of $N(2p^23s\ ^2P)$ was determined to be 98 ± 3 ns. This value agrees well with the literature value, 102 ns.[2] Table 1 compares the present results with the results for the deactivation of $N(2p^23p\ ^4D_{7/2})$ and $Ar(3p^54s\ ^3P_2)$.[7,9] The energies of $N(2p^23p\ ^4D_{7/2})$, 94 882 cm^{-1}, and $Ar(3p^54s\ ^3P_2)$, 93 144 cm^{-1}, are comparable to that of $N(2p^23p\ ^2S)$, 93 582 cm^{-1}.

When Ar was added, the peak height of the VUV emission at 149 nm increased. Although the time integrated intensity of the emission decreased, the Stern–Volmer plot is not linear as is shown in Fig. 2. This suggests that one of the main exit channels in the deactivation by Ar is the production of $N(2p^23s\ ^2P)$. Such an increase in the peak height or the non-linearity in the Stern–Volmer plot was not observed for other quenchers. Since we used an MgF_2 window and an interference filter centered at 150 nm, the emission we observed cannot be attributed to the resonance fluorescence of $Ar(^3P_1–^1S_0)$ at 107 nm or that of $N(^4P_J–^4S_{3/2})$ around 120 nm. The efficiency for the production of $N(2p^23s\ ^2P)$ can be determined by analyzing the Ar pressure dependence of the time-integrated emission intensity. Quenching processes of $N(2p^23s\ ^2P)$ may be neglected, because of its short lifetime.

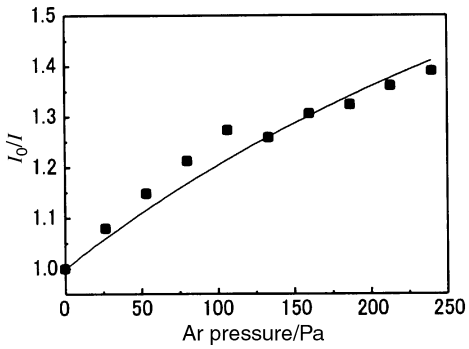

Fig. 2 Ar pressure dependence of the inverse of the VUV fluorescence intensity normalized at the value in the absence of Ar. The smooth curve represents the simulated one with $\alpha = 0.26$.

Table 1 Rate constants for the deactivation of $N(2p^23p\ ^2S)$, $N(2p^23p\ ^4D_{7/2})$, $Ar(3p^54s\ ^3P_2)$ and $N(2p^3\ ^2D)$ in units of 10^{-11} $cm^3\ s^{-1}$

	Rate constant			
Reactant	$N(2p^23p\ ^2S)^a$	$N(2p^23p\ ^4D)^b$	$Ar(3p^54s\ ^3P_2)^c$	$N(2p^3\ ^2D)$
He	<0.02	<0.6		
Ne	0.058 ± 0.003	1.1 ± 1.0		
Ar	25.2 ± 0.5	7.7 ± 1.4		
Kr	27.2 ± 0.3	32 ± 5	0.6	$<0.01^a$
Xe	73.1 ± 1.1	66 ± 12	18	0.72 ± 0.02^a
H_2	46.4 ± 0.8		6.6	0.23 ± 0.02^d
N_2	36.1 ± 0.9	46 ± 6	3.6	0.0013 ± 0.0002^e
CO	60.6 ± 1.7		1.4	0.30 ± 0.02^a
N_2O	78.9 ± 1.5		44	0.22 ± 0.03^f
H_2O	91.2 ± 3.2		48	4.17 ± 0.12^d
CH_4	66.6 ± 0.9		33	0.33 ± 0.02^d
C_2H_6	99.1 ± 3.7		66	2.12 ± 0.16^d
C_3H_8	105.4 ± 4.2		73	3.13 ± 0.31^d
CF_4	26.8 ± 0.9		4	$<0.001^g$
NO	77.6 ± 1.3		22	8.27 ± 0.29^d

[a] This work, [b] Copeland *et al.*,[7] [c] Velazco *et al.*,[9] [d] Umemoto *et al.*,[1] [e] Sugawara *et al.*,[23] [f] Piper *et al.*,[24] [g] Fell *et al.*[25]

Then, the reaction scheme can be represented as follows:

$$N(2p^23p\,^2S) \rightarrow N(2p^23s\,^2P) + h\nu_{IR}; \quad k_1$$

$$N(2p^23p\,^2S) + NO \rightarrow \text{products}; \quad k_2$$

$$N(2p^23p\,^2S) + Ar \rightarrow N(2p^23s\,^2P) + Ar; \quad \alpha k_3$$

$$N(2p^23p\,^2S) + Ar \rightarrow \text{other products}; \quad (1-\alpha)k_3$$

$$N(2p^23s\,^2P) \rightarrow N(2p^3\,^2D) + h\nu_{VUV}; \quad k_4$$

Here, k_j represents the rate constant while α is the efficiency for the production of $N(2p^23s\,^2P)$. It is possible to assume a steady state concentration for $N(2p^23s\,^2P)$ during the decay. The time integrated VUV emission intensity can be expressed by:

$$I_{VUV} \propto (k_1 + \alpha k_3)[Ar])/(k_1 + k_2[NO] + k_3[Ar]).$$

By measuring the Ar pressure dependence of I_{VUV}, it is easy to determine the efficiency, α, since the values of k_1, k_2 and k_3 are known. The smooth curve shown in Fig. 2 represents the non-linear least-squares fit. The corresponding value of α is 0.26. The error limit should be around 10%. In order to check the contribution of pressure broadening, experiments were also carried out in the presence of 27 kPa of He, but there was no large deviation in the best-fit value of α.

Discussion

According to the measurements by Copeland *et al.*, the rate constants for the deactivation of $N(2p^23p\,^4D_{7/2})$ by rare gas atoms increase monotonically with the increase in the atomic weight.[7] There is a similarity between the present result and that of Copeland *et al.* and many parts of their discussion of the deactivation mechanism can be applied in the present system. The efficient quenching by Ar, Kr and Xe can be related to the production of electronically excited rare gas atoms, while such exit channels are closed for He and Ne. However, there is one different point. The rate constant for the deactivation of $N(2p^23p\,^2S)$ by Ar is comparable to that by Kr, while Ar is much less efficient in the quenching of $N(2p^23p\,^4D_{7/2})$ than Kr. In other words, the rate constant for the quenching of $N(2p^23p\,^2S)$ by Ar is exceptionally large. This result was opposite to our expectation. As has been mentioned in the Introduction, in the quenching of $N(2p^23p\,^4D_{7/2})$ by Ar, there are three exothermic exit channels, one of which is near resonant. In the quenching of $N(2p^23p\,^2S)$, on the other hand, only one exothermic channel is available and the energy mismatch is larger. One of the explanations of this result is the production of $Ar(3p^54s\,^3P_1)$. This channel is endothermic, but the endothermicity is only 169 cm^{-1} which can be overcome by the thermal energy. In such a case, some resonance effect may be expected. Of course, transition to the potential curve correlating to $N(2p^3\,^4S) + Ar(3p^54s\,^3P_2)$ should also be important. This point shall be discussed later together with the production mechanism of $N(2p^23s\,^2P)$.

The rate constants for the deactivation of $Ar(3p^54s\,^3P_2)$ are smaller than those of $N(2p^23p\,^2S)$, and possibly $N(2p^23p\,^4D_{7/2})$, especially for diatomic molecules. The small polarizability of $Ar(3p^54s\,^3P_2)$ should be the main cause of the small rate constants.

It is more difficult to explain the efficient production of $N(2p^23s\,^2P)$ by Ar. Such processes have not been identified for other rare gas atoms. The cross-section for the production of $N(2p^23s\,^2P)$ should be as large as 8.5×10^{-16} cm^2, although the production processes are far from resonant:

$$N(2p^23p\,^2S) + Ar \rightarrow N(2p^23s\,^2P_{3/2}) + Ar + 7361\ cm^{-1}$$

$$N(2p^23p\,^2S) + Ar \rightarrow N(2p^23s\,^2P_{1/2}) + Ar + 7444\ cm^{-1}$$

The direct crossing between the potential curves correlating to $N(2p^23p\,^2S) + Ar$ and $N(2p^23s\,^2P) + Ar$ cannot be expected, at least in the long-range region, because the energy difference is too large. Curve crossing at the inner wall region cannot completely be excluded, but that should be less likely because the Σ state correlating to $N(2p^23p\,^2S) + Ar$ should be repulsive, except for a shallow van der Waals well. The contribution of a charge-transfer state is unlikely, also, because both Ar^- and N^- ions are unstable.[14] On the other hand, the potential curves correlating to $N(2p^3\,^4S) + Ar(3p^54s\,^3P_2)$ can be a bridge state to combine the potential curves correlating to $N(2p^23p\,^2S) + Ar$ and $N(2p^33s\,^2P) + Ar$. The C_6 parameter for the attractive part of the Lennard-Jones 6-12 potential can be calculated from the ionization potential and the polarizability.[7] The polarizabilities of $N(2p^23p\,^2S)$ and $Ar(3p^54s\,^3P_2)$ are estimated to be 139×10^{-24} and 47×10^{-24} cm^3 from their ionization potentials,[7] while the polarizabilities of ground-state atoms have been tabulated.[14] The C_6 parameters for $N(2p^23p\,^2S) + Ar$ and $N(2p^3\,^4S) + Ar(3p^54s\,^3P_2)$ pairs are calculated to be 81 and 24 J nm^6 mol^{-1}, respectively. The former potential curve is more attractive and these two curves should cross at a long range. The crossing point is calculated to be 0.47 nm, which is large enough to explain the large cross-section. Fig. 3 illustrates the schematic potential energy diagram of the N–Ar complex. The potential curve correlating to $N(2p^3\,^4S) + Ar(3p^54s\,^3P_2)$ and that correlating to $N(2p^23s\,^2P) + Ar$ may not cross at a long range. However, if one of the Σ or Π states correlating to $N(2p^3\,^4S) + Ar(3p^54s\,^3P_2)$ is attractive, there should be a curve crossing at the inner wall region. The Landau–Zener transition probability should be large in such a case, since the slopes of the potential curves must be similar. As for Kr and Xe, there must be too many exit channels available and the production of $N(2p^23s\,^2P)$ cannot be a major exit channel. There are 9 electronically excited states of Kr below 93 582 cm^{-1}, while there are more than 70 states for Xe.[2,15] A similar process to produce $N(2p^23s\,^4P)$ may be expected in the quenching of $N(2p^23p\,^4D)$ by Ar.

All molecular species examined quench $N(2p^23p\,^2S)$ efficiently without producing $N(2p^23s\,^2P)$. The rate constants for the quenching are determined by long-range interaction potentials and are not controlled by the chemical characters of the quenchers. Correlations between the quenching cross-sections and the long-range interaction parameters have been discussed in many systems, including excited rare gas atoms,[9] excited metal atoms,[8] and excited diatomic hydride molecules.[16–19] The cross-sections for the complex formation can be calculated by a procedure similar to that reported elsewhere.[16,18,20,21] In this model, cross-sections are calculated by assuming multiple attractive interactions and a centrifugal repulsive force. The dispersion interactions is by far the most important among the multipole interactions and the potential was assumed to be represented by $-C_6/r^6$, where r is the

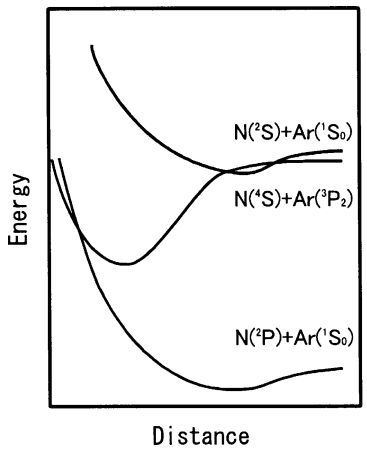

Fig. 3 Schematic potential energy diagram of N–Ar.

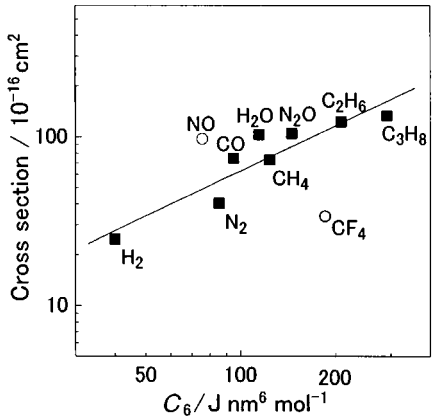

Fig. 4 A log–log plot of the cross-section for the quenching of $N(2p^23p\,^2S)$ *vs.* the long-range interaction parameter, C_6.

intermolecular distance. It was also assumed that a collision complex is formed when the collision pair surmounts the potential barrier. There is a good correlation between the experimentally measured cross-sections and the calculated ones except for two species, NO and CF_4. The correlation is even better when the logarithm of the cross-sections is plotted against the logarithm of the C_6 parameters. The correlation is shown in Fig. 4. The cross-section for NO is larger than expected, while that for CF_4 is smaller. The large cross-section for NO can be explained by taking into account the Penning ionization process besides the energy transfer process. Such a process is allowed only for NO. Perfluoroalkanes are exceptional molecules. The cross-sections for the quenching by CF_4 never exceed those by CH_4, although the polarizability of CF_4 is larger than that of CH_4.[8–11,13,22] The slope of the straight line in Fig. 4 is 0.9. This is in contrast to the theoretical prediction that the slope should be 1/3 if the attractive potential is represented by $-C_6/r^6$.[8] However, this should not be taken seriously, because such discrepancy has been found in many systems.[8] The potential curves may not be represented by simple Lennard-Jones ones.

Conclusions

Nitrogen atoms in the excited $2p^23p\,^2S$ state are quenched efficiently by rare gas atoms and simple molecules except for He and Ne. Since the radiative lifetime of $N(2p^23p\,^2S)$ is relatively long, 102 ns, care must be paid when the densities of the first excited metastable atomic nitrogen, $N(2p^3\,^2D)$, are measured by a two-photon LIF technique. For molecular species except for NO and CF_4, a good correlation was found between the cross-sections and the long-range interaction parameters. In other words, the quenching cross-section can be estimated if the polarizability and the ionization potential are known. Penning ionization may be important in the quenching by NO in addition to energy transfer. The inefficiency in the quenching by He and Ne can be explained by the lack of excited levels below the energy level of $N(2p^23p\,^2S)$. Although the production of $N(2p^23s\,^2P)$ and ground-state rare gas atoms is energetically and symmetrically allowed, there may not be potential curve crossings within the energetically accessible region. On the other hand, for Ar, the potential curve correlating to metastable triplet Ar and ground-state N atoms can be a bridge state to produce $N(2p^23s\,^2P)$ efficiently.

This work was partially defrayed by the Grant-in-Aid for Science Research (No. 11640501) from the Ministry of Education, Science, Sports and Culture of Japan.

References

1 H. Umemoto, N. Hachiya, E. Matsunaga, A. Suda and M. Kawasaki, *Chem. Phys. Lett.*, 1998, **296**, 203.
2 NIST Database for Atomic Spectroscopy.
3 T. Suzuki, Y. Shihira, T. Sato, H. Umemoto and S. Tsunashima, *J. Chem. Soc., Faraday Trans.*, 1993, **89**, 995.
4 Y. Shihira, T. Suzuki, S. Unayama, H. Umemoto and S. Tsunashima, *J. Chem. Soc., Faraday Trans.*, 1994, **90**, 549.
5 G. E. Gadd, L. E. Jusinski and T. G. Slanger, *J. Chem. Phys.*, 1989, **91**, 3378.
6 H. Umemoto and K. Matsumoto, *J. Chem. Soc., Faraday Trans.*, 1996, **92**, 1315.
7 R. A. Copeland, J. B. Jeffries, A. P. Hickman and D. R. Crosley, *J. Chem. Phys.*, 1987, **86**, 4876.
8 W. H. Breckenridge and H. Umemoto, *Adv. Chem. Phys.*, 1982, **50**, 325.
9 J. E. Velazco, J. H. Kolts and D. W. Setser, *J. Chem. Phys.*, 1978, **69**, 4357.
10 V. A. Alekseev and D. W. Setser, *J. Phys. Chem. A*, 1999, **103**, 4016.
11 R. Sobczynski and D. W. Setser, *J. Chem. Phys.*, 1991, **95**, 3310.
12 V. A. Alekseev and D. W. Setser, *J. Chem. Phys.*, 1996, **105**, 4613.
13 V. A. Alekseev and D. W. Setser, *J. Phys. Chem. A*, 1999, **103**, 8396.
14 *CRC Handbook of Chemistry and Physics*, ed. D. R. Lide, CRC, Boca Raton, FL, 76th edn., 1995.
15 C. E. Moore, *Atomic Energy Levels*, Circular of the National Bureau of Standards, Washington, DC, 1958.
16 P. W. Fairchild, G. P. Smith and D. R. Crosley, *J. Chem. Phys.*, 1983, **79**, 1795.
17 R. A. Copeland, M. J. Dyer and D. R. Crosley, *J. Chem. Phys.*, 1985, **82**, 4022.
18 A. Hofzumahaus and F. Stuhl, *J. Chem. Phys.*, 1985, **82**, 3152.
19 R. D. Kenner, S. Pfannenberg, P. Heinrich and F. Stuhl, *J. Phys. Chem.*, 1991, **95**, 6585.
20 H. Umemoto, J. Kikuma, S. Tsunashima and S. Sato, *Chem. Phys.*, 1988, **120**, 461.
21 H. Umemoto, J. Kikuma, S. Tsunashima and S. Sato, *Chem. Phys.*, 1988, **125**, 397.
22 V. A. Alekseev and D. W. Setser, *J. Phys. Chem.*, 1996, **100**, 5766.
23 K. Sugawara, Y. Ishikawa and S. Sato, *Bull. Chem. Soc. Jpn.*, 1980, **53**, 3159.
24 L. G. Piper, M. E. Donahue and W. T. Rawlins, *J. Phys. Chem.*, 1987, **91**, 3883.
25 B. Fell, I. V. Rivas and D. L. McFadden, *J. Phys. Chem.*, 1981, **85**, 224.